A New Horizon for Evaluating Tire Grip Within a Laboratory Environment

Marzieh Salehi[1] · Jacques W. M. Noordermeer[1] · Louis A. E. M. Reuvekamp[2] · Tanya Tolpekina[2] · Anke Blume[1]

Abstract

The evaluation of tire grip on the road is costly and consumes high energy and time, but is essential for safety. Prediction of tire grip on a laboratory scale is therefore always of interest and of utmost importance for research and material developments. It mostly suffers from lack of comparison with actual tire data. To involve all influencing factors on tire grip in a laboratory scale measurement is very complex. Therefore, it has always remained challenging to obtain a strong correlation between laboratory results and road data. In the present study, a new test method is developed for a Laboratory Abrasion Tester, LAT100, which enables to exploit the device as a tribometer. The objective was to develop a technique on a laboratory device to mimic the common test modalities for evaluating tire grip on the road with a trailer tester: lateral (α) and longitudinal (κ) sweep tests. The new method is validated by correlating the laboratory data with the two test modalities of real tire grip on a dry road using a trailer tester for six different tire tread compositions. For the LAT100 tests, solid rubber wheels are characterized at three different normal loads. The effects are comparable with actual tire data. The outcome of the new test method is in good agreement with actual tire trailer α-sweep tests.

Graphical abstract
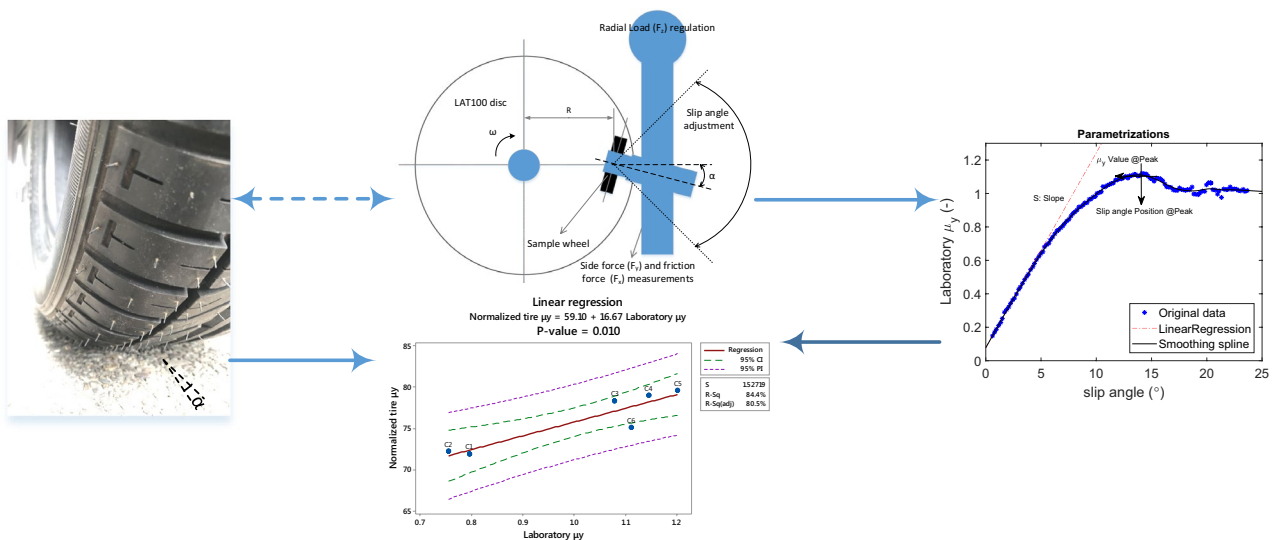
Extended author information available on the last page of the article

1 Introduction

Tire grip or traction is a concept that describes the grasp and interaction between the tire and the road to avoid vehicle skidding or sliding which is crucial for safety. The terms grip or traction both imply the same meaning and can be used interchangeably in this context. Proper tire grip provides a good level of handling which is a prerequisite for vehicle's steering in various driving states such as cornering, braking, and accelerating. The tire grip is the result of the generated frictional forces in the aforementioned driving states which are created by the tire slippage in the contact patch. When a vehicle brakes, accelerates, or corners, the tire tread elements in the contact area move a noticeable displacement in relation to the road. This is called slippage. For instance for an Anti-lock Braking System (ABS), the braking force is optimized based on a specific region of tire slippage to provide adequate frictional forces or grip and avoid tire skidding. This has been elaborated in detail in our previous studies [1, 2]. A tire rolling at a constant speed does not move relative to the road surface in the contact patch, apart from the shear deformations owing to various forms of rolling resistance and carcass (the tire internal structural body except for the tread layer) distortion which creates a very small slippage in the trailing edge. This is beyond the scope of this paper.

Numerous factors influence tire grip: first, the tire construction, tread formulation and the pattern of the tire; second, the road surface characteristics, its condition and structure; and last temperature [3]. The general relationship between the frictional forces and the slippage is a specific characteristic of a tire design that includes the carcass, all rubbers used in the tire structure, and most important the tread. The slippage can be classified in lateral or longitudinal directions based on the driving states. Accordingly, it creates forces that can be categorized in two main modes: lateral

(side) during cornering and longitudinal while braking or accelerating, both with their own specific characteristics.

The lateral force is the force that tires transmit to the ground during cornering in parallel to the rolling axis, see Fig. 1. The angle between the tire plane of symmetry and the actual moving direction of the vehicle in cornering is termed slip angle α (°) which creates lateral slippage. Figure 1 (left) shows atypical relationship between the lateral friction coefficient μ_y and the slip angle. Various lateral forces play a role during tire service, which differ by several orders of magnitude. They encompass cornering forces, camber thrust, and minor residual influences comprised of two components—ply steer (pseudo-slip angle) and conicity (pseudo-camber) [4].

The longitudinal friction force is created when the tire contact patch moves a noticeable displacement in the forward direction during braking or accelerating. The longitudinal slippage is defined by the difference between the forward driving speed and the equivalent circumferential velocity of the wheel [5, 6]. According to the Society of Automotive Engineers (SAE), the longitudinal slip ratio κ is defined as

$$\kappa = -\frac{V_x - R_e\omega}{V_x}, \tag{1}$$

where V_x (m/s) is the longitudinal driving speed and $R_e\omega$ is the equivalent circumferential velocity of the wheel, where ω (rad/s) is the rotational velocity of the wheel and R_e (m) is the effective tire radius. The latter is defined as the radius of the tire when rolling with no external torque applied to the spin axis. Since the tire flattens in the contact patch, this value lies somewhere in between the tire's un-deformed and the static loaded radii [7]. Figure 1 (middle) shows the longitudinal friction coefficient μ_x vs. the negative braking slip ratio according to Eq. 1. Whereas all these phenomena also occur during accelerating conditions, then conversely the slip ratio is positive. Each tire is characterized by a specific
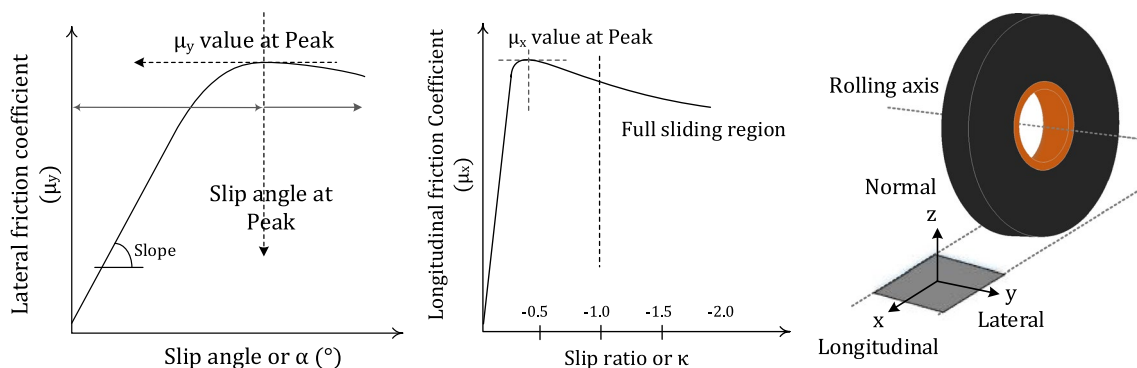
Fig. 1 The general relationships between the frictional forces and the slippage: (left) lateral and (middle) longitudinal braking modes; (right): a sketch of a rolling wheel as a guide for the normal, lateral, and longitudinal directions

friction curve based on its carcass, tread pattern as well as the composition of the various rubber compounds. The typical important parameters of the friction curves are specified in Fig. 1. The slope of the lateral friction at small slip angles, typically smaller than 2–3° for a tire where the friction curve is still linear, represents the cornering stiffness of the tire which originates from tire carcass and tread stiffness.

Accordingly, there are two common methods for assessing tire dry grip. First, lateral (α) sweep in which the α is varied over one complete cycle of slip angle at a specific normal load to the counter-surface at steady speed and a defined camber angle. Second, longitudinal (κ) sweep which is the variation of κ, while maintaining the α equal to zero. The degree of κ is continuously varied by applying a braking force to the wheel. Combined slip is also possible which involves variation of the κ and α simultaneously [8]. During tire tests the lateral and vertical forces and self-aligning torques are collected and by employing the Magic Formula (MF) of Pacejka [9] the data are modeled and presented in the form of the typical graphs as shown in Fig. 1. It is possible to perform the measurements at various normal loads and camber angles.

At automotive and tire industrial companies and institutes, indoor and outdoor test facilities are available for performing full-scale tire measurements to determine tire performances. The outdoor test installations are built on a truck or trailer that is equipped with a special wheel suspension and guidance system to which a measuring hub is attached. Flat track tire testing machines also evaluate tire performances in an indoor laboratory on a full tire on corundum sandpaper. The design of such systems presents a high degree of complexity in order to control the flatness of the rolling surface as well as its dynamic performance to keep it from interfering with the tire [10]. The measurements have a higher precision in comparison with the tire trailer testing because of controlled laboratory environment and conditions, but less accuracy due to the type of test track [11]. At an actual range of loads and speeds of the tire, the flat track tests are not in good agreement with the trailer testing due to the sandpaper substrate which normally becomes saturated with abraded rubber particles which fill out the asperities of the test track. The possibilities of applying a simulated road in the indoor devices have been extensively discussed to obtain proper friction properties [12].

For material development concerning tire performance, both indoor and outdoor tire tests are enormously sophisticated, time-consuming, and costly. It would be highly desirable to predict tire grip performance in a laboratory environment before manufacturing a full tire. Therefore, it is important to evaluate the friction properties which reflect the actual tire grip in a laboratory environment. The evaluated friction properties of the tire tread compound can also be employed as input data for models and simulations for tire characteristics. The quality and parametrization of the tire models and simulations strongly depend on the correct rubber friction properties [13–17]. Tires are built up of a multitude of different elements, mostly rubber compounds, each contributing to the overall performance profile. This complex structure interacts with the road as counter-surface. Therefore, a wide range of factors influences realistic tire grip prediction with determination of the rubber friction in a laboratory environment. Considering all these factors in one laboratory device is a complex task to accomplish.

Many researchers implemented theoretical approaches to describe, understand and calculate friction with respect to influencing parameters such as temperature, rubber formulations and its properties and surface characterization [18–25]. The friction behavior has also broadly been investigated using modeling and simulation by taking parameters such as speed, load, and temperature into account in order to obtain insight into transient friction curves which are difficult to acquire in a laboratory environment [9, 13, 15, 17, 26–29]. On the other side, a large number of testing measurement systems exist that can be classified mainly in two different test set-ups: linear and rotary which are based on the specimen geometry and its relative motion to the counter-surface. The results are commonly expressed in terms of the coefficient of friction [14, 22, 30–38]. ISO 15,113 standard [39] for the frictional properties of rubber was first published in 1999 and is probably the most comprehensive of all friction standards. It was developed from an earlier British standard, BS 903 Part A 61 [40]. The standard methods do not describe a specific apparatus but emphasize the importance of tight control of the various parameters and provides guidance on the factors to be considered in measuring friction. In most mentioned test procedures, the objective is to provide the best correlation with the service conditions, together with good reproducibility between laboratories.

Among all available tribometers suitable for measuring tire tread frictional properties, there is a great interest in measurements with the Grosch wheel [1, 2, 13–17, 28, 31, 41–48]. The main advantage is the rolling movement in the contact area with a renewed surface in each revolution. This helps the rubber to relax in a loading condition similar to a tire which leads to a more realistic temperature profile in the contact area. Using sliding body measurements does not provide a realistic input for tire modeling due to poor surface cooling [13]. Some researchers put more emphasize on the dynamic contact behavior of the rolling wheel because of similarities to the tire by the aid of modeling [13–17].

The Laboratory Abrasion Tester (LAT)100 is one of the machines that is able to simulate a wide range of test conditions in a laboratory environment with a solid rubber sample wheel which was originally developed by Grosch in 1996 [46] to measure the lateral force and the abrasion loss as a

function of various slip angles, loads, and speeds on different counter-surfaces. This apparatus has also been considered for the evaluation of rubber tribological properties due to its similarity to vehicle tire operating conditions [1, 28, 31, 41–46, 48].

For tire grip assessments, so far most attention has been paid to car ABS braking distance data, especially on wet surfaces. Good agreements have been acquired with laboratory tribometers, both linear and rotary measurements, with ABS braking data. A Linear Friction Tester (LFT) provides a strong correlation with outdoor ABS data on wet [49] and snow surfaces [50], but not for dry surfaces primarily because of poor temperature control in the contact area [49]. The portable LFTs provide the possibility to perform in-situ measurements on the actual testing fields or road surfaces. Some good agreements have been reported between LAT100 results and ABS braking data on different surfaces [1, 31, 48].

In the present study, the prediction of tire grip on a dry surface is investigated in a laboratory environment with a LAT100, compared with the friction curves acquired from actual tire grip data in the two driving states of cornering and braking. Basically, the objective was to apply and simulate α- and κ-sweep tests of the trailer tire testing in the laboratory device. A new test method is developed for the LAT100 by which the instrument can be utilized as a tribometer to generate the full friction curve. New dynamic functions are defined which enable one to work in a semi-automatic mode of the LAT100 machine. This allows to program the LAT100 parameters: slip angle, load, and speed with time. The test method is designed in such a way that it needs substantially shorter test times in comparison with the conventional measuring method of the LAT100. This method is verified and validated with actual tire data on a dry road, evaluated with a tire trailer tester with two test modalities of κ and α sweeps for a wide range of tread compounds. Corresponding solid rubber wheels are characterized on the modified LAT100 on a specific electro-corundum counter-surface with a particular grain size based on our earlier study [1], disc 180 of the LAT100 (see later). The experiments are performed at three different normal loads and the effects are compared between laboratory and tire samples. The results are in a good agreement primarily with the actual tire trailer α-sweep tests.

The advantage of the current study is first the comparison and correlation of laboratory data with the actual tire data on the road, and secondly the design of a unique method analogous to the tire situation on a laboratory scale for the evaluation of the rubber properties and the acquisition of full friction curves. This method also reduces the change of the rubber sample surface during the measurement which stems from the inherent rubber abrasion during the measurements for acquiring the friction curves. The test results

are comprehensively validated for a large variety of rubber compounds and test conditions.

2 Experimental

2.1 Tire Data Generation

2.1.1 Tread Compounds

Six passenger tread compounds C1 to C6 were designed comprising various types of carbon black and silica fillers with different particle sizes; C1 to C3 were pure silica reinforced, C4 was based on a blend of silica and carbon black, and C5 and C6 on pure carbon black. This was expected to provide a significant difference in tire grip. The reason for this wide selection was to strengthen the laboratory method validation in the current study.

To prepare full tires from experimental compounds for tire trailer testing on the road, large amounts of such compounds are needed. Each compound needs to be extruded to the green tread dimension according to its specification. Considering the different rheological behaviors of the compounds, various die designs would be required. Consequently, it is not time- and cost-effective to extrude the full treads in a tire production line. Therefore, experimental tires were prepared via treads which were prepared in a laboratory environment. To prepare these treads, the rubber compounds were calendered and rolled into the particular width and assembled according to the specification of the tire size 235/35R19 slick. Full-size tires were manufactured with the same construction process using the same body components, but with the prepared treads. To compare tire data and calculate the rating, an additional proprietary reference compound was used and considered as the standard tire.

2.1.2 Tire Tests

The two types of tire tests that were performed were κ and α sweep tests as explained in Sect. 1, on an asphalt testing field with a test trailer. The tests were carried out at a constant speed of 60 km/h and at three different normal load settings: 3430, 4910 and 6870 N (corresponding to 350, 500, and 700 kg, respectively). The slip condition depending on the type of test mechanism differs. The α-sweep tests were performed from $-12°$ to $+12°$ slip angle with a slip rate of $2°/s$. The κ-sweep tests were performed at a constant slip angle α of $0°$ and the κ varied in a range of 0 to -0.45 in the braking mode. For α-sweep tests the lateral forces F_y and for κ-sweep tests the longitudinal friction forces F_x were collected. The experiments were executed randomly for all the tires with the various compounds with 3 times repetition for
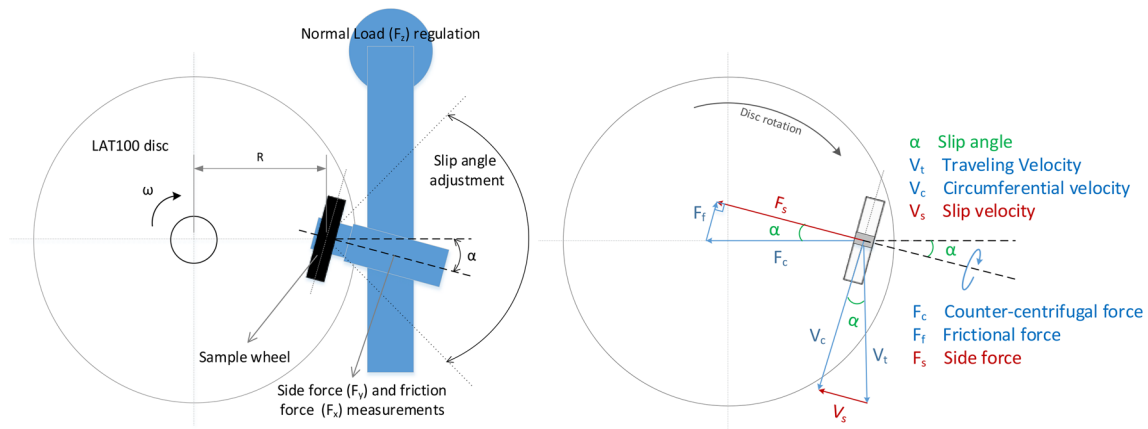
Fig. 2 Schematic views of the measurement unit of the LAT100

the reference tire. The camber or inclination angles in these experiments are less than 0.5°, which is negligible.

2.2 Laboratory Data Generation

2.2.1 Test Set-Up

The used laboratory set-up is known with the commercial name LAT100 manufactured by VMI Holland B.V., the Netherlands. The details of the test set-up were fully described in our previous manuscript [1]. The measurement unit consists of a solid rubber test wheel which is pressed under a vertical load of $F_z(N)$ normal to a driven disc as the counter-surface. The circumferential velocity of the test wheel V_c is induced by the disc traveling velocity, $V_t = R \times \omega$ where R is the distance of the disc center to the center of the rubber wheel contact patch and ω (rad/s) is the rotational

velocity of the disc. The average slip velocity V_S in the contact area is created by combining traveling velocity and slip angle, α, which for the center point of the test wheel in contact with the disc is given by

$$V_s = V_t \times \sin \alpha. \tag{2}$$

The resultant forces are generated by the slip velocity and the acting normal force. A schematic view of the measurement unit and the trigonometry of the velocities and resultant forces in the center of the contact patch: F_c counter-centrifugal force, F_y lateral force, and F_x friction force are represented in Fig. 2. The coordinate system is considered to be linked to the center of the rubber wheel.
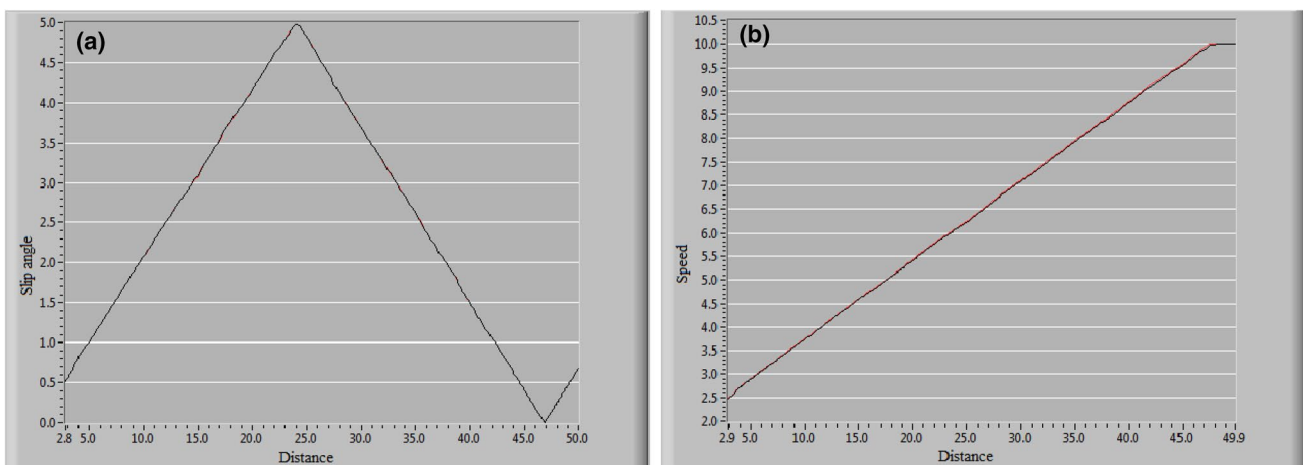

Fig. 3 Modified LAT100 software illustrating: **a** a triangular function of slip angle (°); and **b** a ramp function of speed (km/h) vs. distance (m)

2.2.2 New Test Design

Within this study, a new test method was designed for the aforementioned test set-up. The conventional LAT100 could only be operated with static set points for the input parameters—disc traveling speed, normal load, slip angle—which had to be defined and imported in the machine software before each test run. The software was modified so as to be able to control the machine in a dynamic way in which the input parameters vary during the test runs based on defined functions to specified set points. The input parameters change vs. traveling distance or time with a pre-defined mathematical function with which the tire conditions on the road can be transformed to the rolling rubber wheel. For instance, Fig. 3 shows two examples of different dynamic functions of the modified LAT100 software; (a) slip angle as a triangular function of distance; and (b) speed as a ramp function of distance. Any combinations of the three input parameters with the dynamic functions are an option. It is also possible to program the test set-up in a way which allows one to simulate non-stop runs of different test conditions on one rubber test wheel. This allows to simulate the actual tire behaviors on the road in a series of test conditions and evaluate the rubber compound properties in a set of functions and test conditions resembling real tires. The test time is greatly decreased and the experiments can be performed within minutes in comparison with at least one full day with the conventional LAT100 method. It also reduces the change of the rubber sample surface which is caused by abrasion during the measurements while acquiring the friction curves.

2.2.3 The Test Track

The employed laboratory test disc was based on our previous study [1] and provided by VMI Holland BV Tire Industry Equipment. It is composed of electro-corundum white Al_2O_3 powder bound in a ceramic binder with a weight ratio of 85/15%. The grain size distribution of the used powder is the percentage of individually sized particles contained in the designated grit sizes and classified with the code 180 according to ISO525:2013(E), as given in Table 1. The corundum particles in the ceramic binder are pressed together and the disc surfaces flattened by a grinding process using fine steel powder. The surface root mean square S_q of the disc roughness was measured on an area of 1414 μm × 1080 μm as given in Table 1; A microscopic image of the disc surface was obtained with confocal laser scanning microscopy VK 970 Keyence.

Table 2 Experimental conditions on disc 180 in laboratory device

Parameters	Experimental conditions
Loads (N)	55, 75 and 95
Speeds (km/h)	0.2, 2.1, 6.5, 11
Distance (m)	0.91, 9.5, 29.5, 50
Angle rate (°/s)	1.53
Slip angle (°)	Sweep from 0 to 25

Table 1 Characterizations of the laboratory test track: disc coded 180 of LAT100

Disc designation	180	Microscopic image
Disc code	EKW 180 SHARP	
Particle size (μm)	60	
Corundum sieve analysis (μm)	0% > 125 Maximum 15% > 90 Minimum 40% > 63 Minimum 65% > 53	
S_q (μm)	96	

2.2.4 The Rubber Test Wheel Samples

From all tire tread compounds, laboratory rubber test wheels with external diameter of 84 mm and thickness of 19 mm were vulcanized in a Wickert laboratory press WLP 1600 for 11 min at 170 °C under a pressure of 160 bar, optimized on basis of t_{90} cure meter data. Finally, the samples were stored for 12 h at room temperature, 22 °C $\pm$ 1 °C. Therefore, the initial temperatures of all samples were equal when starting the laboratory experiments.

2.2.5 Test Conditions

For realistic and repeatable evaluations, some pre-conditioning test runs on a brand-new rubber sample and disc track were performed to remove the shiny outer vulcanization skin from the rubber wheel samples and level the sharp asperities of the experimental track, like the test conditions described in [1]. After every single test for each slip angle, disc cleaning was performed using an air pressure nozzle

Table 3 Tire μ_x ratings at peaks of the tire κ-sweep friction curves for different loads

	Tire μ_x at peaks		
	350 kg	500 kg	700 kg
C2	101.4	97	98.4
C3	102.4	100.3	100.4
C1	100.7	98.7	96.1
Average of all refs	100	100	100
C4	97.9	96	96
C5	93.8	92.8	89.6
C6	92.8	90	90.3
CV (%) ref	2.2	2.1	2.1

which removed the rubber debris and particles from the disc surface. The linear function of the slip angle vs. traveling distance of the LAT100 is the closest operating test condition compared to the described tire tests in Sect. 2.1.2. Hence, for the angle rate (°/s) which is the rate of slip angle α change with time or rather with distance traveled, the following relation with the conventional parameters of the LAT100 holds:

$$\text{angle rate} (°/s) = \frac{\text{Slip angle} (°) \times \text{Speed} (m/s)}{\text{Distance} (m)}. \tag{3}$$
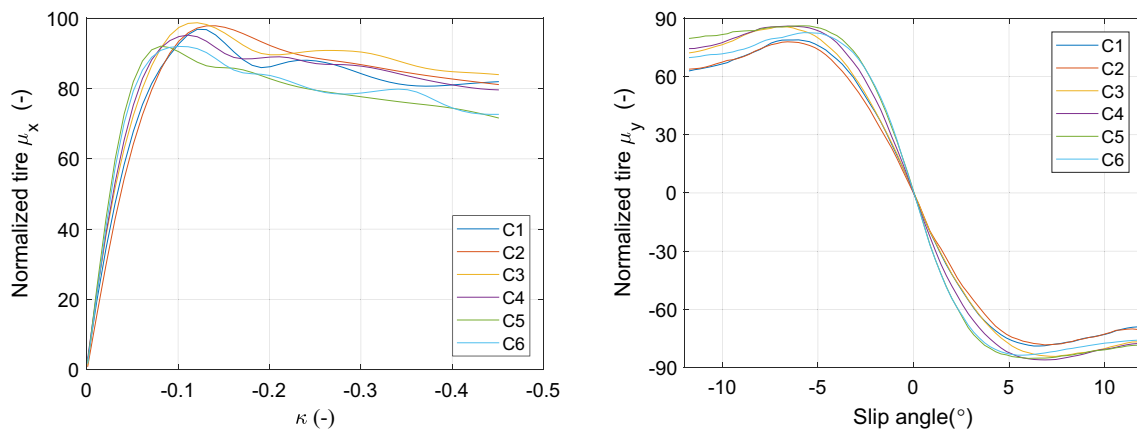
The lateral forces were evaluated under the applied normal load, slip angle, and traveling velocity V_t to determine the friction curve which is represented as μ_y according to

$$\mu_y = \frac{F_y(N)}{F_z(N)}. \tag{4}$$

The ranges of speeds and loads as covered within the defined test conditions are listed in Table 2. The traveled distances are calculated according to Eq. 3 for a constant angle rate of 1.53°/s for each test condition. 1.53°/s of the angle rate is the optimized value based on the available machine setting to obtain a full friction curve within the range of defined variables. The speed range was based on "scaling down" the angular speed of the tested tire size (235/35R19) to the laboratory test wheel [51]. The speed, slip angle, and angle rate was calculated to get close to the tire service condition in the contact area using this scaling model. The ratio of the tire to the test wheel circumferences is around 8. Therefore, the equivalent speed for the test wheel was estimated to be of order 8 times smaller compared to a speed of 60 km/h for the tire tests. Therefore, a range of 4 speeds from 0.2 km/h to 11 km/h was employed.

Fig. 4 Normalized tire friction curves of the trailer tests at 350 kg load, (left) κ-sweep and (right) α-sweeps

Table 4 Tire μ_y ratings at Min. and Max. points and the slope S at 0° of the tire α-sweep friction curves for different loads

	Tire μ_y at Max	Tire μ_y at Min	S(slope) at 0°
350 kg			
C2	92.8	92.9	76.5
C3	101.1	100.2	84.4
C1	93.3	94.0	85.0
Average of all refs	100.0	100.0	100.0
C4	101.0	102.5	100.4
C5	101.3	101.3	116.1
C6	97.3	99.2	119.4
CV (%) ref	1.0	0.5	2.0
500 kg			
C2	92.7	93.5	74.9
C3	101.0	98.3	79.9
C1	93.3	93.3	80.2
Average of all refs	100.0	100.0	100.0
C4	99.2	99.3	93.8
C5	97.4	98.5	109.7
C6	95.2	98.4	111.2
CV (%) Ref	1.6	0.1	3.2
700 kg			
C2	93.0	91.9	78.6
C3	101.1	99.2	82.9
C1	92.9	91.5	85.0
Average of all refs	100.0	100.0	100.0
C4	102.2	100.8	95.4
C5	103.1	100.4	100.1
C6	97.2	98.3	114.2
CV (%) Ref	0.4	0.5	3.1

3 Results and Discussion

3.1 Tire Test Data

3.1.1 κ-Sweep Tests

The tire μ_x value, see Fig. 1, is obtained by dividing the longitudinal braking friction force by the normal load F_x/F_z. Table 3 shows the tire μ_x ratings at Peaks of the friction curves in the κ-sweep tests; the Peak point is identified in Fig. 1. The compounds are rated based on the average values of the reference compound. The rating of the reference compound is set at 100%. The data are presented for the three different applied loads. The Coefficients of Variation (CV)—the ratio of standard deviation to the mean—of the reference compound were calculated corresponding to each load setting as also shown in Table 3 to provide an impression of the repeatability of the tests. An example of a κ-sweep friction curve at 350 kg for the tested compounds
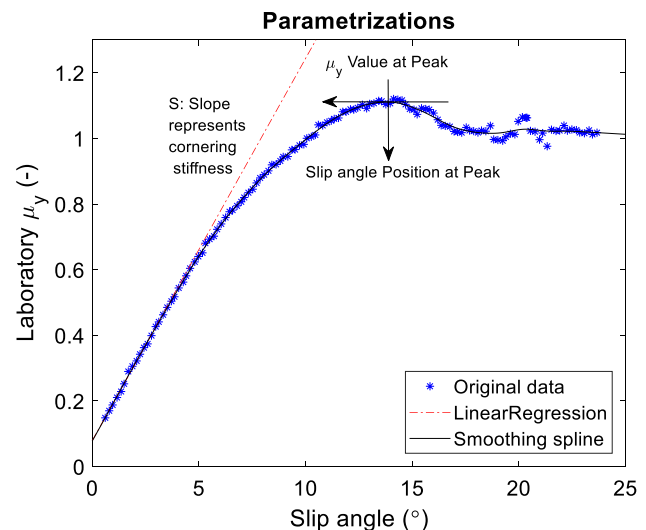
Fig. 5 Example of a friction curve prepared by the modified LAT100 for C2 at speed 2.1 km/h and load 55 N; dashed line: the linear regression at small slip angles, arrows: peak position on slip angle axis and the corresponding μ_y value

is illustrated in Fig. 4 (left) which is the normalized tire μ_x versus the slip ratio κ. All the μ_x values are normalized by dividing by the largest μ_x value of the reference compound and are expressed in percentage.[1]

3.1.2 α-Sweep Tests

Tire μ_y is obtained by dividing the lateral force to the normal load F_y/F_z versus slip angle α(°). Figure 4 (right) shows an example at 350 kg load of the α-sweep friction curves for the tested tread compounds. All the μ_y values are normalized as carried out for the μ_x values, by dividing by the largest μ_x value of the reference compound. By this approach the magnitudes of the normalized μ_y are comparable with the normalized μ_x values. The data including slope S at 0°, the minimum tire μ_y value (tire μ_y at Min.), the maximum tire μ_y value (tire μ_y at Max.) of the α-sweep friction curves, and the CVs for the reference compounds are represented in Table 4.

3.2 Laboratory Results with the Modified LAT100

The generated slip velocity with the LAT100 is based on varying the slip angle. Previously [1], the friction curves

---

[1] Actual tire data were considered to be proprietary. The point we try to make here is that the ranking of the tire data and laboratory results are similar. With this point, we validate the new laboratory technique. We support this with the statistical analysis of P-values and R-sq, as specified later in Figure 11. By doing so, the order of magnitude of normalized numbers are still comparable and the final results remain the same.
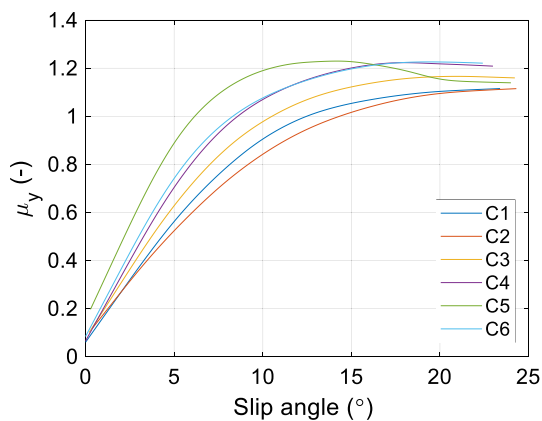
Fig. 6 Examples of laboratory μ_y vs. Slip angle (°) for all compounds in the modified LAT100

Table 5 Regression coefficients R^2 between the tire data ratings at three different tire loads

Tire loads	350 kg	500 kg	700 kg
R^2 between κ-sweep μ_x at peak & α-sweep μ_y at Max.	0.08	0.11	0.03
R^2 between κ-sweep μ_x at peak & α-sweep μ_y at Min.	0.20	0.02	0.04

were provided in a static mode where the traveling speeds, loads, and slip angles remained constant during a test run. In the present study, the experiments were carried out by varying the slip angle as a single dynamic linear function of distance based on the new test modality. This present test method is similar to the tire α-sweep test which provides a higher control of the abrasion and surface temperature of the test wheel in comparison with the single point measurement
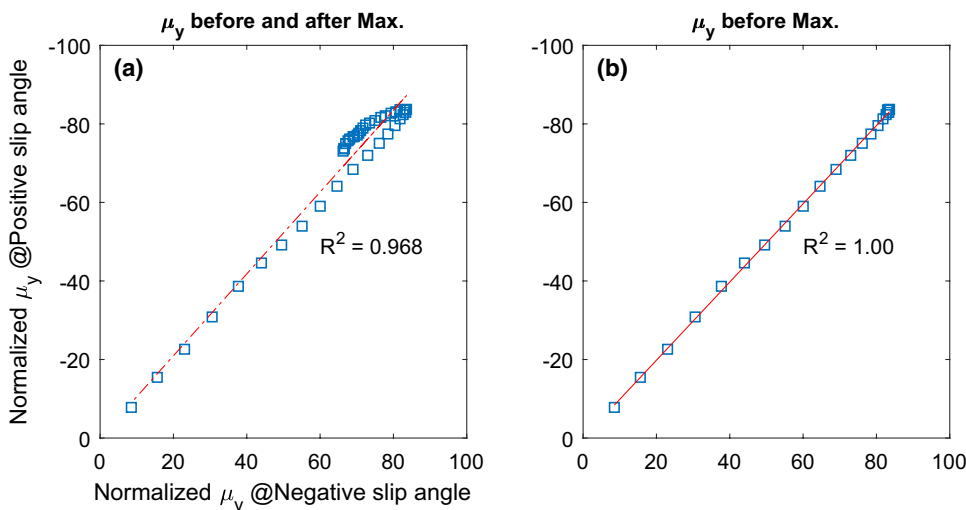
method. The test time is greatly decreased and the experiments can be performed within seconds. An example of the generated friction curves by the newly designed modality is presented in Fig. 5. The best way for parametrization of the friction curves is applying models like the MF of Pacejka [9]. Data filtering was performed using Matlab R2017b by exploiting smoothing spline functions: see Fig. 5. In mathematics, a spline is a function defined piecewise by polynomials. The spline is preferred over polynomial interpolation because it yields a good fitting. Accordingly, the slip angle position on the x-axis at Peak, μ_y value at Peak, and at last the slope S at small slip angles can be derived by a linear regression below 5° for LAT100.
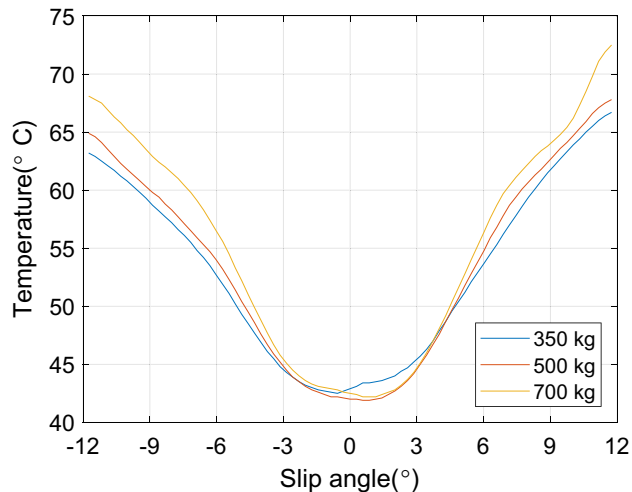
The repeatability of the laboratory sweep tests was also investigated. The CV for the μ_y at Peak for the reference compound was measured as 1.2% which is comparable to the tire data: see Table 3 and 4. At higher slip angles, e.g., 25º the abrasion and high temperature create 1% more variation in the laboratory results. All sweep experiments with the modified LAT100 were performed under the test conditions mentioned in Table 2. After data smoothing for the output friction curves, the results were correlated with the collected tire data, see Sect. 3.4. Examples of smoothed μ_y vs. Slip angle (°) for the modified LAT100 for the various tested compounds at speed 6.5 km/h and 55 N load are presented in Fig. 6.

3.3 Tire Data Analysis

Before validating the new technique and correlating the laboratory results with the actual tire data, it is necessary to investigate the relation—if any—between the two different test modalities of α- and κ-sweep of the tire data for all six tread compounds. Both test modalities were outdoor types and the friction behaviors were measured on full-scale tire interfaces with the same road asphalt surface. Therefore,

Fig. 7 μ_y at negative vs. positive slip angles for the reference compound at load 350 kg

Table 6 Correlation coefficients R^2 between μ_y values at positive and negative slip angles for different loads

Loads (kg)	R^2
350, 500	0.90
350, 700	0.91
500, 700	0.89

Fig. 8 Tire tread surface temperatures in a sweep from −12 to 12° for the Reference compound

coefficients R^2 were calculated for different normal loads. The R^2 values for the correlations between α- and κ-sweep tests are very poor: see Table 5. This indicates that the compound with the superior longitudinal grip in the κ-sweep test does not offer the best behavior in the lateral direction of the α-sweep test: see Fig. 4. It suggests different contributions of friction mechanisms: adhesion and hysteresis, that govern the contact between the tire and asphalt. It is therefore worthwhile to investigate how the different test mechanisms adversely affect the grip properties of longitudinal and lateral slippage mainly after the peak. It demonstrates that the two test modalities need to be looked at each on their own. This will be covered in a separate paper.

3.3.1 Symmetry of Tire α-Sweep Tests

In order to properly analyze the tire data, it is important to judge whether the α-sweep curves are symmetrical. The tire μ_y values in the mirrored α-ranges: negative and positive slip angles, per each load for all compounds were correlated. Figure 7 shows an example of the correlated μ_y values at the positive slip angle vs. the negative slip angle for the reference compound at load 350 kg. If the curves were perfectly symmetrical, the R^2 values should be 1.0. The R^2 value of 1.0 value before the Max. and Min. points of the friction curves demonstrates full symmetry. Given the uncertainties in performing the tests beyond the Max. and Min. points where sliding occurs, the curves are not fully symmetrical, although the ratings of the respective compounds in the positive and negative ranges of slip angle are still correlated: see Fig. 7a.

Another approach is to correlate the tire data, comparing the μ_y values for different applied normal loads. The correlation coefficients R^2 are given in Table 6, which demonstrates that even with different loads the friction behaviors remain reasonably well correlated.

the comparison between the acquired tire data demonstrates the difference in the two tire test modalities. As discussed in Sect. 1, the differences between these test modalities are the slippages based on different displacement types and directions of tread elements: longitudinal and lateral, with their generated forces. For the κ-sweep test, the slip ratio is calculated based on Eq. 1 and for the α-sweep the slip angle is considered.
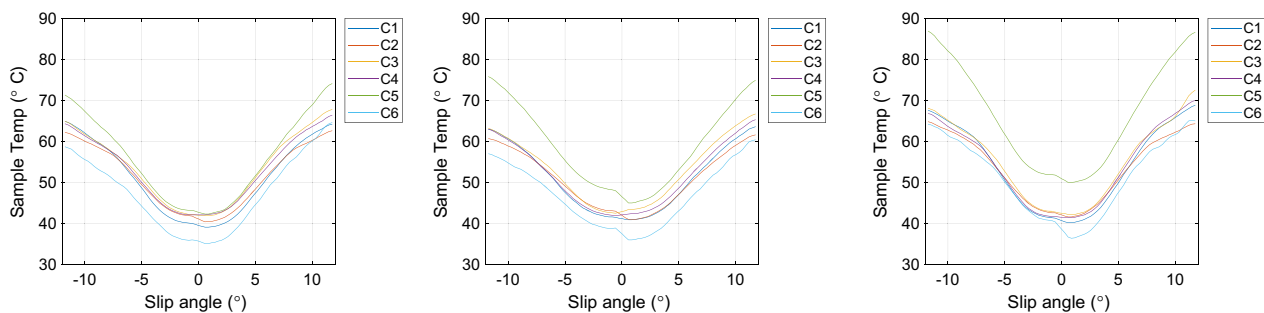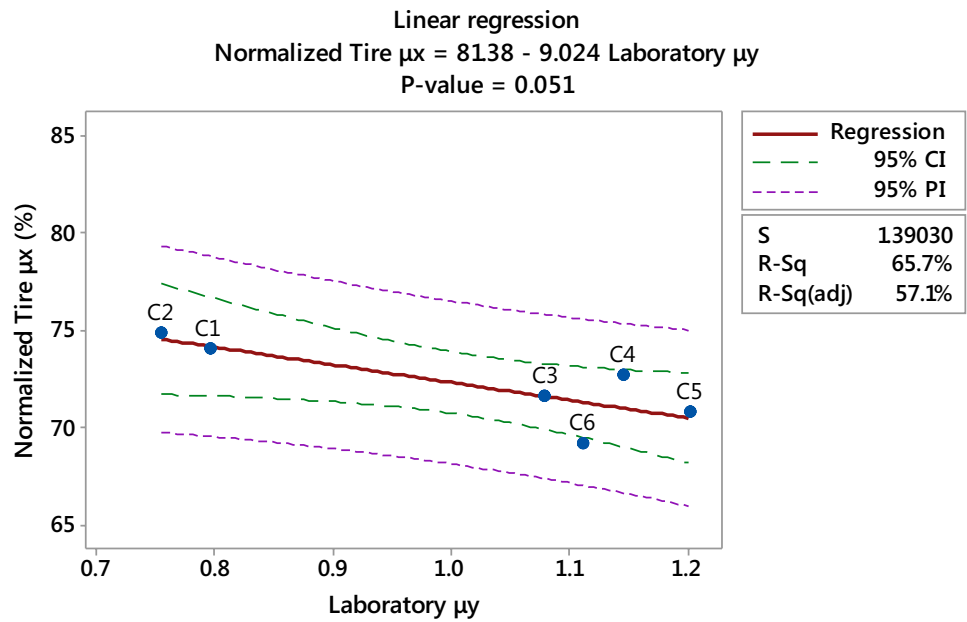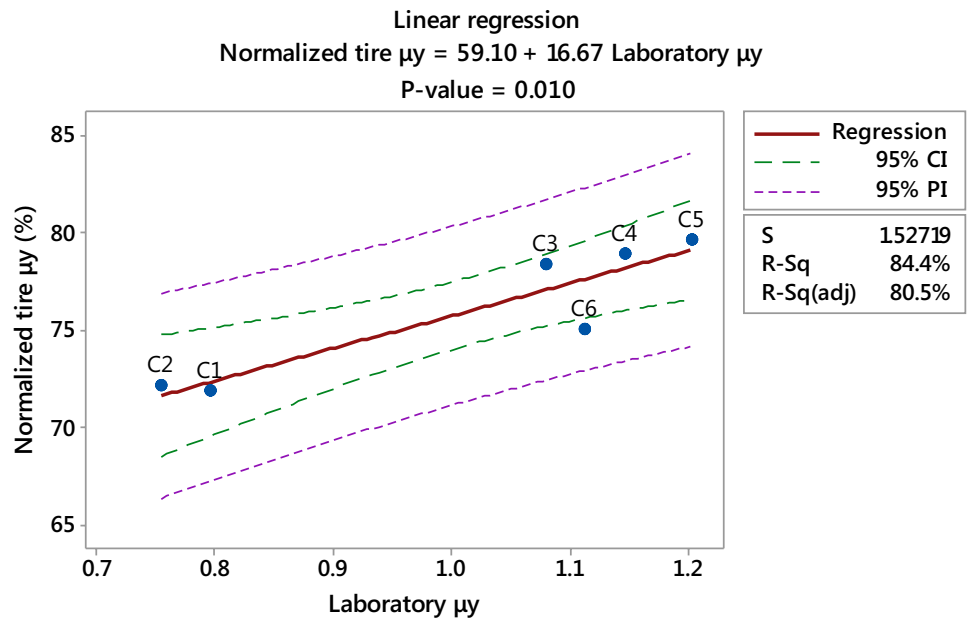
In order to check eventual correlations, the tire μ_y values at the Max. and Min. points of the α-sweep curves were plotted on a linear scale vs. the μ_x values at Peak of the κ-sweep curves, as derived from Fig. 4. The regression
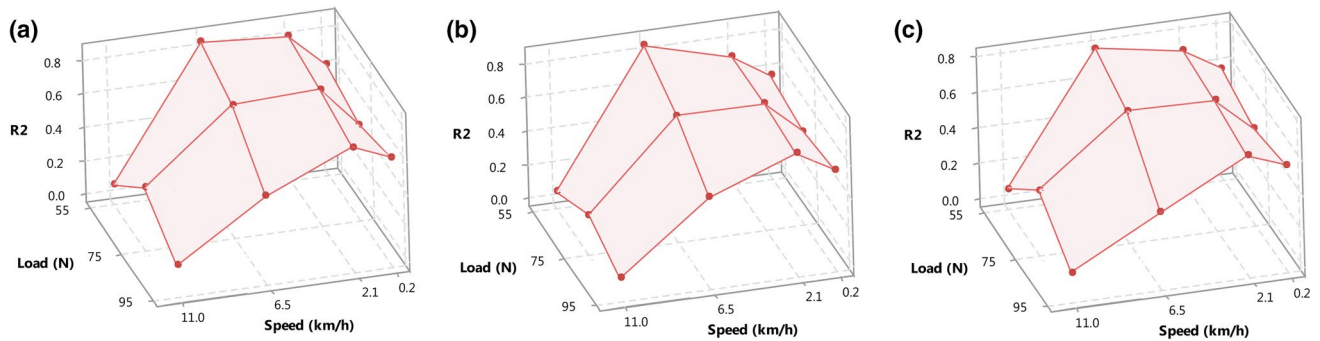

Fig. 9 Temperatures from the trailer α-sweep tests at different loads for all tread compounds: 350 kg, 500 kg, and 700 kg from left to right, respectively; tire testing at constant speed of 60 km/h according to Sect. 2.1

Fig. 10 Examples of the correlation between friction coefficients at peaks of the normalized tire α-sweep (up) and κ-sweep (down) tests with laboratory results

Linear regression
Normalized tire µy = 59.10 + 16.67 Laboratory µy
P-value = 0.010

Regression	
95% CI	
95% PI	
S	152719
R-Sq	84.4%
R-Sq(adj)	80.5%

Linear regression
Normalized Tire µx = 8138 - 9.024 Laboratory µy
P-value = 0.051

|	
Regression	
95% CI	
95% PI	
S	139030
R-Sq	65.7%
R-Sq(adj)	57.1%

Table 7 Calculated R^2 values according to Fig. 10, for comparison between the tire μ_y values from α-sweep data and laboratory μ_y values at Peak for all test conditions

		Tire load (kg)	**Laboratory results**											
	Figure 11		Speed (km/h)	0.2			2.1			6.5			11		
			Load (N)	55	75	95	55	75	95	55	75	95	55	75	95
Tire α-sweep tests	a	350	R² values:	0.61	0.53	0.61	**0.81**	0.77	0.70	**0.85**	0.75	0.48	0.07	0.33	0.14
	b	500		0.57	0.51	0.56	0.71	0.71	0.69	**0.85**	0.71	0.50	0.05	0.19	0.09
	c	700		0.58	0.50	0.56	0.71	0.69	0.64	**0.79**	0.70	0.39	0.07	0.32	0.12
	d	350		0.55	0.45	0.54	0.71	0.72	0.54	0.67	0.69	0.27	0.19	0.44	0.26
	e	500		0.34	0.25	0.33	0.54	0.58	0.37	0.54	0.52	0.18	0.28	0.29	0.34
	f	700		0.56	0.47	0.51	0.63	0.62	0.53	0.63	0.63	0.21	0.12	0.51	0.17

Fig. 11 Graphical representations of Table 7 Rows a, b, c: the regression coefficients R^2 (z-axis) vs. load and speed of the laboratory results; the R^2 values are based on correlations between the tire μ_y values at Min. of the α-sweep tests at different tire loads: **a** 350 kg, **b** 500 kg, and **c** 700 kg, and the μ_y values at Peak for the laboratory results
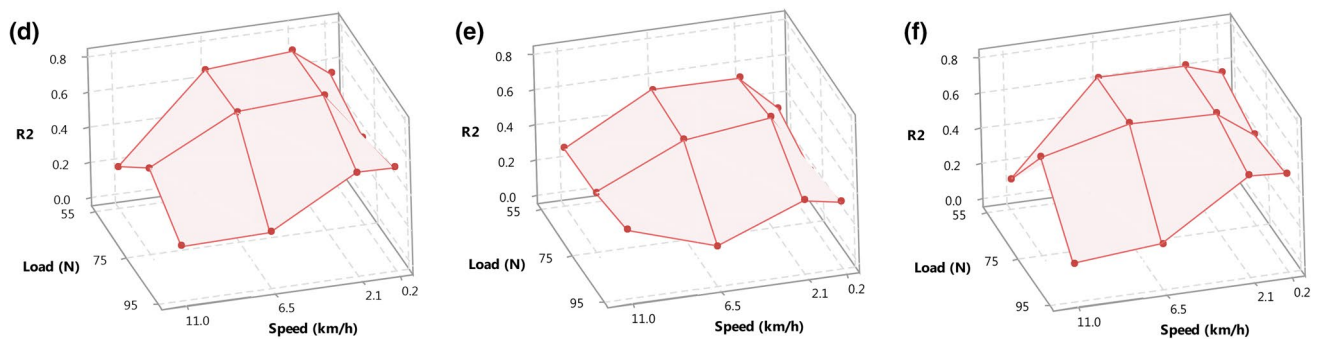
Fig. 12 Graphical representations of Table 7 Rows d, e, f: the regression coefficients R^2 (z-axis) vs. load and speed of the laboratory results; the R^2 values are based on correlations between the tire μ_y values at Max. of the α-sweep tests at different tire loads: **d** 350 kg, **e** 500 kg, and **f** 700 kg, and the μ_y values at Peak for the laboratory results

3.3.2 Tire Temperature

The tire temperature profiles in a half circle sweep from $-12°$ to $12°$ for different applied loads are shown in Fig. 8. The temperature drops by the sweep from $-12°$ to $0°$ and rises again when it reaches slip angle $12°$. By increasing load, the temperature profile shifts upward to higher temperatures. The temperatures from the trailer α-sweep test at different loads for all tread compounds are presented in Fig. 9. For every sweep from $-12°$ to $12°$, the temperature profiles are similar for each compound but slightly higher for C5 due to its special application. When the tire direction is changed from negative to positive slip angles, the abrasion pattern of the tread compounds also changes. This leads to non-symmetrical α-sweep curves. The temperature profiles presented in the current context were recorded with outdoor tire testing within two days. The reader also is referred to Table 10 in the supplementary data for further comparisons.

3.4 Validation of the Laboratory Technique in Comparison with the Road Data

3.4.1 The Validation Approach

After all the preparatory work, the laboratory method can now be validated with the analyzed tire data. The approach to validate the new technique is by correlating the two groups of the collected data in the laboratory and on the road; the 6 test wheels vs. the 6 tire samples at all test conditions. The fitting parameters derived from the friction curves of the tire data in Tables 3 and 4 and the laboratory results in, e.g., Figure 5 were correlated linearly. Examples of linear regression between the tire trailer α- or κ- sweep tests and the modified LAT100 results for all compounds are shown in Fig. 10. The high correlation coefficient R^2 for the α-sweep test indicates that the relative ranking of the measured μ_y for the six compounds on laboratory scale with the new technique is similar to the tire data on the road. The regression slopes of the figures for α- and κ-sweep tests with laboratory results are opposite of one another, indicating that

Table 8 Calculated R^2 values for comparison between the tire α-sweep data and laboratory results for slope S at all test conditions

Tire load	Slope at 0° for Tire α-sweep	Laboratory results for S at small slip angles										
	Speed (km/h)	0.2			2.1			6.5			11		
	Load (N)	55	75	95	55	75	95	55	75	95	55	75	95
350 kg		0.91	0.86	0.41	0.87	0.84	0.78	0.86	0.86	0.56	0.89	0.90	0.77
500 kg	R^2 values	0.94	0.86	0.47	0.90	0.88	0.68	0.90	0.89	0.61	0.90	0.89	0.74
700 kg		0.70	0.79	0.14	0.61	0.57	0.58	0.60	0.60	0.26	0.71	0.79	0.80

the new test set-up of the modified LAT100 only correlates with the tire trailer α-sweep tests with positive slopes; the higher the μ_y in the laboratory, the higher the μ_y on the road. The positive slopes between the LAT100 and tire α-sweep data emphasize the similarities between both test mechanisms. The P value of the linear regression between the tire μ_y and laboratory μ_y is smaller than 0.05 which attributes to a statistically significant correlation within a 95% confidence interval; this is not the case for the regression between tire μ_x and laboratory μ_y as indicated in Fig. 10. The negative slopes of the correlation with the κ-sweep does not have a physical meaning in the present context. All slopes for all tested conditions are summarized in Table 11 in the supplementary data.

It should be noted though that the data of the full-scale tire tests, i.e., α- and κ-sweeps interfacing with the same asphalt as the counter-surface, already could not be correlated as explained in Sect. 3.3 of the tire data analysis, see Table 5. As indicated before in Sect. 2.2.1, the slippage in the contact area of the laboratory test wheel and the tire in α-sweep test are both lateral. Still considering the vast selected range of rubber tread compounds for the present study, the prediction of actual tire lateral grip on the road with a solid test wheel within a laboratory environment is highly successful. However, the argument of the effect of different types of slippage by the two test modalities on friction should be investigated further.

3.4.2 Correlations Between Laboratory Results and Tire Data

To explore the interaction between load and speed in laboratory measurement conditions in Table 2 on prediction of the tire α-sweep tests, the validation approach of Sect. 3.4.1 was employed to all laboratory and tire test data. The regression coefficients R^2 between the μ_y values at Max./Min. of the tire α-sweeps and the μ_y values at Peak for the modified LAT100 sweep tests are summarized in Table 7. Each value in Table 7 shows the calculated R^2 for all six compounds like in Fig. 10. 3D graphical representations of the correlation coefficients are presented in Figs. 11 and 12; which shows where the interaction of two factors of load and speed results in the occurrence of the strong correlations.

Where the R^2 values are the highest, the relative rankings of the measured μ_y for the six compounds with the new laboratory technique are closest to tire data on the road. For the laboratory experimental parameters, the speed has a quadratic influence on the R^2 values, vs. the load with a linear impact. Therefore, the speed is the most significant and the effect of normal load is less pronounced compared to the influence of speed. The dependency of the coefficient of friction on speed was also demonstrated by Grosch to be quadratic, where he showed the similarity to the viscoelastic properties tan δ of the rubber [52].

The R^2 values are largest for speed around 6.5 km/h. The scaling down of the traveling speed of the tested tire size (235/35R19) to the laboratory test wheel, as explained in section test conditions, was estimated to be around 8 times smaller compared to a speed of 60 km/h for the tire tests. The present results validate the scaling down of the tire radius to the laboratory test wheel. The contact and relaxation times of the rubber elements in each revolution of the tire and laboratory wheel are similar. This concept is more clear by elaborating on basis of the well-known tire brush model [53]: the volume of rubber of the tread in the contact area is assumed to be a number of deformable elastic bristles that touch the counter-surface. The time lapse between when a bristle leaves the contact area until it comes in contact again will approximately be the same between the tire and the test wheel. That provides a bristle or rather a volume element of the tread the same time to relax from deformation at similar angular velocity. It implies that analogous test mechanisms and dynamics on the road and in the laboratory scale are generated. Therefore, the comparison can be narrowed down mainly to the rubber tribological properties of the tread compound of the tire and test wheel.

3.4.3 Correlations of Cornering Stiffness

Additional to correlating the tire μ_y values at Max./Min. and laboratory μ_y value at Peak, the so-called cornering stiffness represented by the S (slope) at 0° of the tire α-sweep data and the S at small slip angles for the laboratory μ_y curves can also be correlated: see Fig. 5 for the slope. The calculated R^2 values are presented in Table 8. The tire cornering stiffness stems mainly from the tread compound stiffness because

the structure of all tested tires is the same. For the solid test wheels, the radial thickness represents the cornering stiffness. Also higher load directly affects R_e which leads a drastic change for the calculated R^2 values. So, the correlations for slope S become worse at the higher loads of tires and test wheels, which shows the limit to the load ranges that can be applied.

3.4.4 Visual Comparisons Between Road and Laboratory

A point to mention still is the fact that the R^2 values for correlation with the μ_y at Max. are somewhat lower than the μ_y at Min. The reason is that the friction curves for the α-sweep tests are not fully symmetrical as already explained in Sect. 3.3, Fig. 7. This is a consequence of the way the α-sweep tests on the real tires are executed. It comes from the temperature and the abrasion pattern in the contact area of the tire with the road in the sliding regions of the friction curves. However, there are not only the correlations between

the μ_y at Max. and Min. of the tire data and μ_y at Peak of the laboratory results, the whole friction curves are comparable with the tire data, compare Figs. 6 and 13.

For a better visualization, the α-sweep curves of Fig. 4 (right) were split in two parts: positive and negative slip angles and replotted in a right-handed Cartesian coordinate system. An example is shown in Fig. 13 for the six compounds for load 350 kg. By comparing the laboratory results and the tire α-sweep data at different loads, the effect of the normal load on the tires and the LAT100 test samples is shown to be similar. An example of this trend at speed 6.5 km/h is shown in Fig. 14 for compound C4; see the supplementary data for the rest of compounds at different experimental test conditions.

As to the influence of different tire loads on the R^2 values in Table 7, the laboratory results are correlating satisfactorily with the minimum tire α-sweep data at all loads at the speed of 6.5 km/h. This is due to the fact that the tire data themselves already correlated well among themselves
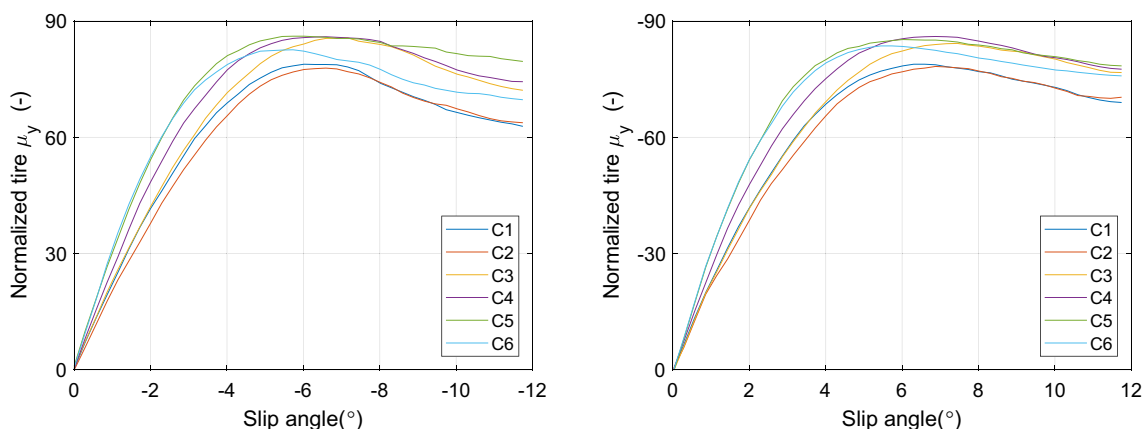

Fig. 13 Splitting and replotting the α-sweep curves of the normalized tire data in a right-handed Cartesian coordinate system for the load 350 kg
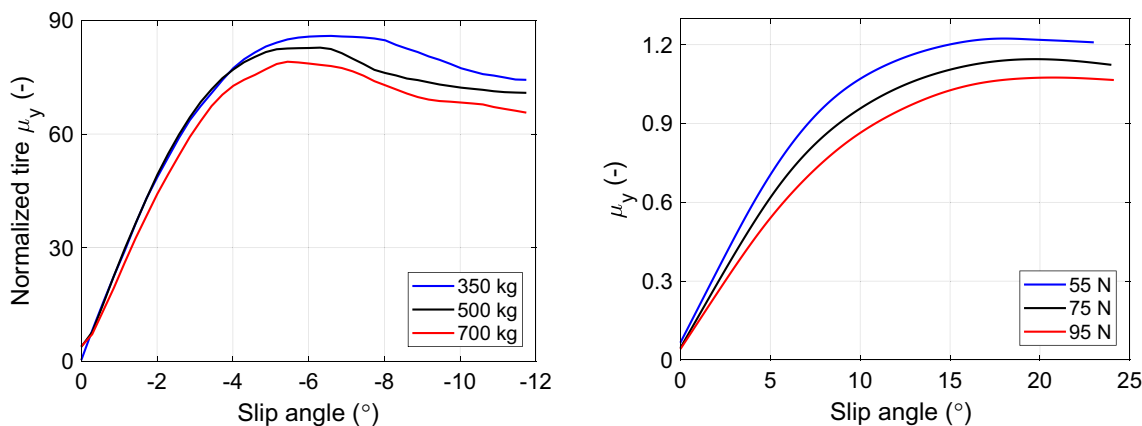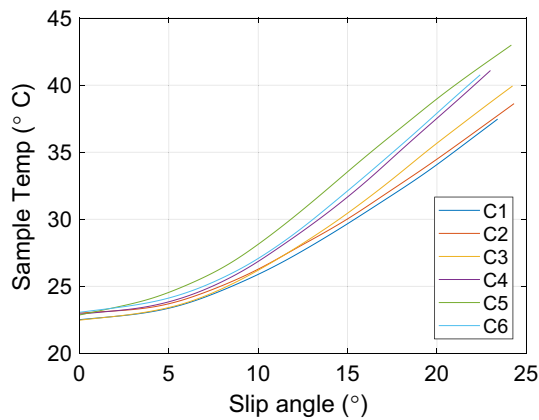

Fig. 14 Comparing (left) the normalized tire data with (right) laboratory results at speed 6.5 km/h at different loads for compound C4

Fig. 15 An example of the surface temperature profiles of the 6 compounds at speed 6.5 km/h and 55 N load

at different loads: see Table 6. The effect of normal load is less pronounced compared to the influence of speed. This corresponds with Schallamach and Grosch who showed that the proportionality of the friction coefficient to the normal load is of a power − 1/3 for a smooth surface to − 1/9 for a rough one [54, 55]: so the effect is limited than speed. Moreover, the larger load also decreased the R_e in Eq. 1 of the test wheel. That explains the poorer correlation at higher load in the laboratory results, e.g., for 95 N.

3.4.5 Temperature Effect

Figure 15 demonstrates the temperature profiles for LAT100 sweeps at load 55 N and speed 6.5 km/h for all compounds. The final surface temperatures of the test wheels for different compounds as presented in Table 9 are slightly lower than the tire temperatures in Supplementary Table 10. The speed has again more influence on temperature rise rather than load.

3.4.6 Concluding Remarks

Above all, the lateral forces measured with the laboratory test method are solely expected to be the cornering forces; compared to tire α-sweep tests the total collected lateral forces are comprised of major cornering forces and minor contributions of camber thrust and residual influences of ply steer and conicity from the tire structure. Given the large differences between the full-scale tires with air inside and the solid rubber test wheels in the laboratory, and the many influencing factors involved, the correlation coefficient of 0.844 in Fig. 10 for the modified LAT100 test method on the laboratory track, i.e., the disc 180 for this vast range of rubber compounds, is a surprisingly satisfactory correlation and as discussed statistically significant, provided the proper experimental conditions are applied based on the scaling-down model as presented here above. This shows the utmost importance of modeling the small solid rubber wheel in the lab and compare it with the tire load distribution to obtain an insight into the different ranges of slip angles in x-axes of Figs. 6 and 13. This will be the subject of a future study.

4 Conclusions

Prediction of tire grip on a laboratory scale is always of interest and of high importance for research and material developments. In the present study, a new test method was developed for a Laboratory Abrasion Tester, (LAT100) in which the device is exploited as a tribometer with the aim of mimicking the common test modalities of evaluating the tire grip on the road with a trailer tester: lateral (α) and longitudinal (κ) sweep tests. For validation, the new test method was compared with tire grip data collected with the two modalities of a trailer tester on a dry test track for six different tire tread compositions.

Table 9 The final sample temperatures of the laboratory wheels at different speeds and loads

Load (N)	Speed (km/h)	C1	C2	C3	C4	C5	C6
55	0.2	23	24	24	23	24	24
	2.1	27	29	28	29	32	30
	6.5	39	40	38	41	43	41
	11	49	50	50	49	51	46
75	0.2	25	24	24	24	24	24
	2.1	28	29	29	30	32	31
	6.5	41	45	42	46	45	45
	11	54	56	56	54	59	53
95	0.2	23	24	23	23	23	23
	2.1	29	30	30	31	33	32
	6.5	42	42	45	49	54	45
	11	54	59	57	55	61	56

- Correlation for the α-sweep tests (lateral slip, i.e., "cornering grip") were found to be strong (R^2 value > -0.84; P value < 0.05 and a 95% of confidence interval).
- The R^2 values for the correlations between tire α- and κ-sweep tests on the road are poor. Consequently, the correlations for the κ-sweep tests (longitudinal slip, i.e., "acceleration and braking grip") were not found in agreement with the laboratory test set-up.
- Benchtop testing for ranking of lateral slip performance over a range of loads and speeds can be conducted in only 1 min, compared with months of preparation and trailer testing of real tires.
- The correlation coefficients are the strongest, based on scaling down of the tire radius to the laboratory test wheel. The condition of appr. 7 km/h and 55 N load on the benchtop tester gives the best correlation with 60 km/h and 350 kg load for α-sweep tests on the tire trailer tester.
- Given the large differences between the full-scale tires with air inside and the solid rubber test wheel in the laboratory, the obtained correlations for this vast range of rubber compounds are surprisingly satisfactory, provided the proper experimental conditions are applied based on the scaling-down model as presented.
- Additional work is required to better understand the two different modalities involved in tire slippage in lateral and longitudinal directions on the road, to be able to also propose new scaling rules for the longitudinal slip on a laboratory benchtop test.
- The approach described to predict actual dry tire grip as a function of speed and load with this laboratory device offers a positive new horizon to evaluate tire grip.

References

1. Salehi, M., Noordermeer, J.W.M., Reuvekamp, L.A.E.M., Dierkes, W.K., Blume, A.: Measuring rubber friction using a Laboratory Abrasion Tester (LAT100) to predict car tire dry ABS braking. Tribol Int **131**, 191–199 (2019). https://doi.org/10.1016/j.triboint.2018.10.011

2. Salehi, M.: LAT100. Prediction of tire dry grip. University of Twente, Enschede (2017)

3. Grosch, K.: Some factors influencing the traction of radial ply tires. Rubber Chem. Technol. **57**(5), 889–907 (1984). https://doi.org/10.5254/1.3536047

4. Pacejka, H.B.: Chapter 4—semi-empirical tyre models. In: Tyre and Vehicle Dynamics, 2nd edn.. pp. 156–215. Butterworth-Heinemann, Oxford (2006)

5. Rajamani, R.: Lateral and longitudinal tire forces. Vehicle Dynamics and Control. Mechanical Engineering Series, pp. 387–432. Springer, US (2012)

6. Majerus, J.N.: Your tire's behavior. In: Winning More Safely in Motorsports; the Workbook. pp. 268–283. Racing vehicle Inc., (2007)

7. Miller, S.L., Youngberg, B., Millie, A., Schweizer, P., Gerdes, J.C.: Calculation longidudinal wheel slip and tire parameters using GPS velocity. American Control Conference, Arlington **3**, 25–27 (2001)

8. Pacejka, H.B.: Chapter 12 - Tyre steady-state and dynamic test facilities. In: Tyre and Vehicle Dynamics, 2nd edn. pp. 586–594. Butterworth-Heinemann, Oxford (2006)

9. Bakker, E., Nyborg, L., Pacejka, H.B.: Tyre modelling for use in vehicle dynamics studies **196**, 190–204 (1987)

10. Cabrera, J., Ortiz, A., Simón, A., García, F., Pérez, A., Perez-Blanca, A.: A versatile flat track tire testing machine a versatile flat track tire testing machine **40**, 271–284 (2003)

11. Ludwig, C.: Influence of testing surface on tire lateral force characteristics. In: Science meets Tires, Aachen 2018, p. 14. ika INSTITUT FÜR KRAFTFAHRZEUGE and RWTH AACHEN UNIVERSITY

12. Christian Carrillo, C.B.: Can we get the road into the lab? Challenges in tire tesing. In: Science meets Tires, Aachen, Germany 2018. ika INSTITUT FÜR KRAFTFAHRZEUGE and RWTH AACHEN UNIVERSITY

13. Riehm, P., Unrau, H.-J., Gauterin, F.: A model based method to determine rubber friction data based on rubber sample measurements. Tribol Int **127**, 37–46 (2018). https://doi.org/10.1016/j.triboint.2018.05.039

14. Bouzid, N., Heimann, B.: Micro texture characterization and prognosis of the maximum traction between Grosch wheel and asphalt surfaces under wet conditions. In: Besdo, D., Heimann, B., Klüppel, M., Kröger, M., Wriggers, P., Nackenhorst, U. (eds.) Elastomere Friction: Theory, Experiment and Simulation, pp. 201–220. Springer, Berlin (2010)

15. Bouzid, N., Heimann, B., Trabelsi, A.: Empirical friction coefficient modeling for the Grosch-wheel-road system. In: VDI Berichte. pp. 291–307. (2005)

16. Gutzeit, F., Kröger, M.: Experimental and theoretical investigations on the dynamic contact behavior of rolling rubber wheels. In: Besdo, D., Heimann, B., Klüppel, M., Kröger, M., Wriggers, P., Nackenhorst, U. (eds.) Elastomere Friction: Theory, Experiment and Simulation, pp. 221–249. Springer, Berlin (2010)

17. Dorsch, V., Becker, A., Vossen, L.: Enhanced rubber friction model for finite element simulations of rolling tyres. Plast. Rubber Compos. **31**(10), 458–464 (2002). https://doi.org/10.1179/146580102225006486

18. Persson, B.N.J.: Theory of rubber friction and contact mechanics. J. Chem. Phys. **115**(8), 3840–3861 (2001). https://doi.org/10.1063/1.1388626

19. Lorenz, B., Oh, Y.R., Nam, S.K., Jeon, S.H., Persson, B.N.J.: Rubber friction on road surfaces: experiment and theory for low sliding speeds. J. Chem. Phys. **142**(19), 194701 (2015). https://doi.org/10.1063/1.4919221

20. Kanafi, MM., Tuononen, A.J., Dorogin, L., Persson, B.N.J.: Rubber friction on 3D-printed randomly rough surfaces at low and high sliding speeds. Wear **376**, 1200–1206 (2017). https://doi.org/10.1016/j.wear.2017.01.092

21. Persson, B.N., Albohr, O., Tartaglino, U., Volokitin, A.I., Tosatti, E.: On the nature of surface roughness with application to contact mechanics, sealing, rubber friction and adhesion. J. Phys. Condens. Mat: Inst. Phys. J. **17**(1), 1–62 (2005). https://doi.org/10.1088/0953-8984/17/1/r01

22. Klüppel, M., Heinrich, G.: Rubber friction on self-affine road tracks. Rubber Chem. Technol. **73**(4), 578–606 (2000). https://doi.org/10.5254/1.3547607

23. Heinrich, G., Klüppel, M.: Rubber friction, tread deformation and tire traction. Wear **265**(7), 1052–1060 (2008). https://doi.org/10.1016/j.wear.2008.02.016

24. Feshanjerdi, M., Khorrami, M., Masoudi, A.A., Razzaghi Kashani, M.: The hysteretic contribution of friction for the polished rubber on the concrete surface. Appl. Surf. Sci. **394**, 528–533 (2017). https://doi.org/10.1016/j.apsusc.2016.10.054

25. Salehi, M., Razzaghi-Kashani, M.: Comparing styrene butadiene rubber–clay nanocomposites prepared by melt intercalation and latex-coagulation methods. J. Appl. Polym. Sci. **126**(1), 253–259 (2012). https://doi.org/10.1002/app.36980

26. Svendenius, J.: Review of wheel modeling and friction estimation. Lund Inst, Technol (2003)

27. Erdogan, G.: Tire modeling, lateral and longitudinal tire forces. (2009).

28. Steen, R.v.d., Lopez, I., Nijmeijer, H.: Experimental and numerical study of friction and .giffness characteristics of small rolling tires. Tire Sci. Technol. **39**(1), 5–19 (2011). https://doi.org/10.2346/1.3555134

29. Kane, M., Cerezo, V.: A contribution to tire/road friction modeling: from a simplified dynamic frictional contact model to a "Dynamic Friction Tester" model. Wear **342**, 163–171 (2015). https://doi.org/10.1016/j.wear.2015.08.007

30. Brown, R.: Friction and wear. In: Physical Testing of Rubbers. pp. 219–243. Springer (2006)

31. Heinz, M., Grosch, K.A.: A laboratory method to comprehensively evaluate abrasion, traction and rolling resistance of tire tread compounds. Rubber Chem. Technol. **80**(4), 580–607 (2007). https://doi.org/10.5254/1.3548182

32. Mihajlovic, S., Kutscher, U., Wies, B., Wallaschek, J.: Methods for experimental investigations on tyre-road-grip at arbitrary roads. Internationale Konferenz ESAR "Expertensymposium Accid. Res." (2013).

33. Germann, S., Wurtenberger, M., Daiss, A.: Monitoring of the friction coefficient between tyre and road surface. In: *1994 Proceedings of IEEE International Conference on Control and Applications, 24–26* Aug 1994 1994, pp. 613–618 vol. 611

34. Najafi, S.: Evaluation of continuous friction measuring equipment (CFME) for supporting pavement friction management programs. Virginia Tech (2010)

35. Lindner, M., Kröger, M., Popp, K., Blume, H.: Experimental and analytical investigation of rubber friction. *Paper Presented at the ICTAM04 Proceedings*, Warsaw, Poland,

36. Lahayne, O., Eberhardsteiner, J., Reihsner, R.: Tribological investigations using a linear friction tester (LFT). Transact. FAMENA **33**(2), 15–22 (2009)

37. Krasmik, V., Schlattmann, J.: Experimental investigation of the friction and wear behaviour with an adapted ball-on-prism test setup. Tribol. Industr. **37**(3), 291–298 (2015).

38. Pacejka, H.B.: Chapter 2—basic tyre modelling considerations. In: Tyre and Vehicle Dynamics (2nd edn.). pp. 61–89. Butterworth-Heinemann, Oxford (2006)

39. ISO 15113: Rubber. In: Determination of Frictional Properties. (2005)

40. BS903-A61: Physical testing of rubber—determination of the frictional properties of rubber. In: Rubber and Plastic industries: British Standards Institution, (1994)

41. Nguyen, V.H., Zheng, D., Schmerwitz, F., Wriggers, P.: An advanced abrasion model for tire wear. Wear **396**, 75–85 (2018). https://doi.org/10.1016/j.wear.2017.11.009

42. Wu, J., Zhang, C., Wang, Y., Su, B.: Wear predicted model of tread rubber based on experimental and numerical method. Exp. Tech. **42**(2), 191–198 (2018). https://doi.org/10.1007/s40799-017-0214-1

43. Grosch, K.A.: Correlation Between road wear of tires and computer road wear simulation using laboratory abrasion data. Rubber Chem. Technol. **77**(5), 791–814 (2004). https://doi.org/10.5254/1.3547852

44. Grosch, K.A.: Goodyear medalist lecture. rubber friction and its relation to tire traction. Rubber Chem. Technol. **80**(3), 379–411 (2007). https://doi.org/10.5254/1.3548172

45. Grosch, K.A.: Rubber abrasion and tire wear. Rubber Chem. Technol. **81**(3), 470–505 (2008). https://doi.org/10.5254/1.3548216

46. Grosch, K.A.: A new way to evaluate traction-and wear properties of tire tread compounds: paper presented at the Rubber Division, American Chemical Society, Cleveland, Ohio, 21–24 October

47. Heinz, M.: A laboratory abrasion testing method for use in the development of filler systems. Technical report rubber reinforcement systems (2015).

48. Heinz, M.: A universal method to predict wet traction behaviour of tyre tread compounds in the laboratory. J. Rubber Res. **13**(2), 91–102 (2010)

49. Ignatyev, P.A., Ripka, S., Mueller, N., Torbruegge, S., Wies, B.: Tire ABS-braking prediction with lab tests and friction simulations. Tire Sci. Technol. **43**(4), 260–275 (2015). https://doi.org/10.2346/tire.15.430401

50. Ella, S., Formagne, P.-Y., Koutsos, V., Blackford, J.R.: Investigation of rubber friction on snow for tyres. Tribol. Int. **59**, 292–301 (2013). https://doi.org/10.1016/j.triboint.2012.01.017

51. Salehi, M., Noordermeer, J.W.M., Reuvekamp, L.A.E.M., Blume, A.: A new method to rapidly predict tyre grip in a laboratory environment. In: International Rubber Conference, London, UK, 3–5 2019

52. Grosch, K.A.: The relation between the friction and viscoelastic properties of rubber. Rubber Chem. Technol. **37**(2), 386–403 (1964). https://doi.org/10.5254/1.3540331

53. Pacejka, H.B.: Chapter 3—theory of steady-state slip force and moment generation. In: Tyre and Vehicle Dynamics (2nd edn.). pp. 90–155. Butterworth-Heinemann, Oxford (2006)

54. Grosch, K.A., Schallamach, A.: The load dependence of laboratory abrasion and tire wear. Rubber Chem. Technol. **43**(4), 701–713 (1970). https://doi.org/10.5254/1.3547282

55. Schallamach, A.: The load dependence of rubber friction. Proc. Phys. Soc. B **65**, 657–661 (1952)

Affiliations

Marzieh Salehi[1] · Jacques W. M. Noordermeer[1] · Louis A. E. M. Reuvekamp[2] · Tanya Tolpekina[2] · Anke Blume[1]

✉ Marzieh Salehi
  m.salehi@utwente.nl

✉ Jacques W. M. Noordermeer
  j.w.m.noordermeer@utwente.nl

[1] Department of Elastomer Technology and Engineering, University of Twente, P.O. Box 217, Enschede 7500, The Netherlands

[2] Apollo Tires Global R&D B.V., Colosseum 2, Enschede 7521, The Netherlands